Astronomy & Astrophysics

The nature of the fluorescent iron line in V 1486 Orionis

S. Czesla and J. H. H. M. Schmitt

Hamburger Sternwarte, Universität Hamburg, Gojenbergsweg 112, 21029 Hamburg, Germany
e-mail: stefan.czesla@hs.uni-hamburg.de

ABSTRACT

The fluorescent 6.4 keV iron line provides information on cool material in the vicinity of hard X-ray sources as well as on the characteristics of the X-ray sources themselves. First discovered in the X-ray spectra of the flaring Sun, X-ray binaries and active galactic nuclei (AGN), the fluorescent line was also observed in a number of stellar X-ray sources. The young stellar object (YSO) V1486 Ori was observed in the framework of the *Chandra* Ultra Deep Project (COUP) as the source COUP 331. We investigate its spectrum, with emphasis on the strength and time variability of the fluorescent iron K_α line, derive and analyze the light curve of COUP 331 and proceed with a time-resolved spectral analysis of the observation. The light curve of V 1486 Ori shows two major flares, the first one lasting for $\approx$20 ks with a peak X-ray luminosity of 2.6×10^{32} erg/s (dereddened in the 1−10 keV band) and the second one – only partially observed – for >60 ks with an average X-ray luminosity of 2.4×10^{31} erg/s (dereddened). The spectrum of the first flare is very well described by an absorbed thermal model at high temperature, with a pronounced 6.7 keV iron line complex, but without any fluorescent K_α line. The X-ray spectrum of the second flare is characterized by even higher temperatures ($\gtrsim$10 keV) without any detectable 6.7 keV Fe XXV feature, but with a very strong fluorescent iron K_α line appearing predominantly in the 20 ks rise phase of the flare. Preliminary model calculations indicate that photoionization is unlikely to account for the entire fluorescent emission during the rise phase.

Key words. stars: early-type – stars: activity – X-ray: stars

1. Introduction

The COUP data set provides a nearly continuous 13 day long X-ray observation of the Orion nebula star forming region and is currently one of the best suited data sets for the exploration of the X-ray properties of large and homogeneous samples of young stars. Substantial analysis of this data set has already been performed (e.g. by Getman et al. 2005). In particular, Tsujimoto et al. (2005) carried out a systematic search for the occurrence of the fluorescent iron K_α line at 6.4 keV, identifying 7 COUP sources with detectable fluorescent emission. This emission line is particularly interesting since it can provide a wealth of information on the emitting source(s). Fluorescent 6.4 keV photons – hereafter referred to as Fe I K_α photons – result from a de-excitation of neutral or lowly ionized iron atoms, following an excitation leaving the iron ion with a K-shell vacancy. When the latter is filled by another (mostly L-shell) electron, the excess energy can be carried by a fluorescent photon. Highly ionized iron can also show this behavior, but the transition energy rises because of the reduced screening of the inner electrons from the nuclear charge. Several processes lead to the ejection of a K-shell electron and, thus, to the creation of the Fe I K_α line. During the process of photoionization a K-shell electron is ejected from iron after the absorption of a photon with an energy exceeding 7.11 keV. Alternatively, high energy particles can eject K-shell electrons with the same threshold energy.

The first detection of the fluorescent Fe I K_α line was reported in the context of solar physics (e.g. Neupert et al. 1967). A model succeeding in explaining most of the solar Fe I K_α emission with photoionization only was proposed and

evaluated by Bai (1979), yet, e.g., Zarro et al. (1992) argue that photoionization alone is not sufficient to account for all of the solar Fe I K_α emission. Fluorescent K_α line emission has also been reported from other celestial X-ray sources. It is typically encountered in the high-energy emission from AGN and X-ray binaries, which are characterized by high X-ray luminosities and rather hard X-ray spectra, thus providing large photon numbers above the 7.11 keV threshold for photoionization. Fabian et al. (1989) detect the fluorescent iron line in the spectrum of the X-ray binary Cyg-X1, and Tanaka et al. (1995) were the first to report the relativistically broadened line in the spectrum of the AGN MCG-6-30-15. Recent observations with XMM-*Newton* and *Chandra* extended the class of Fe I K_α line emitters to a number of stellar sources, such as the class I YSO Elias 2-29 (Favata et al. 2005), the above seven COUP sources discussed by Tsujimoto et al. (2005), and the YSO YLW 16A for which Imanishi et al. (2001) carried out time-resolved spectroscopy.

In this letter we present a detailed analysis of the X-ray properties of the YSO V 1486 Ori (=COUP 331) with emphasis on its Fe I K_α emission, which was already reported by Tsujimoto et al. (2005), who measured a normalization of $2.6(0.1-4.6) \times 10^{-7}$ ph/(cm^2 s) with an equivalent width of 126 eV for the fluorescent line. Unfortunately, the YSO V 1486 Ori has so far not received much attention at other energy bands. From the 2MASS-all-sky survey we infer its infrared magnitudes as 12.5 mag, 10.6 mag, and 9.4 mag, in the J, H, and K_s bands, respectively. Tsujimoto et al. (2005) show that the infrared colors of V 1486 Ori do not match the regions of reddened dwarfs or giants and argue for the presence of a NIR-emitting inner disk. Moreover a rotation period of (6.09 ± 0.3) d is known for
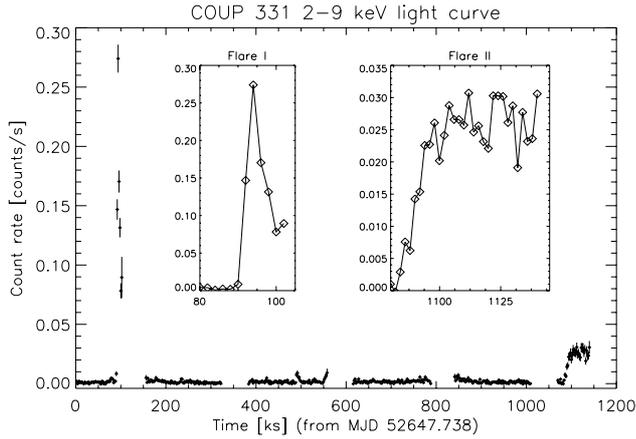
Fig. 1. Background-subtracted light curve of COUP 331 with 2 ks binning. Inserted panels show close-up views of the flares I and II.

Fig. 2. Spectrum of COUP 331 during flare I (*upper curve*) and the quiescent phase (*lower curve*), both fitted with an absorbed VAPEC model.

V 1486 Ori (Herbst et al. 2002; Stassun et al. 1999). Following Tsujimoto et al. (2005) we adopt a distance of 450 pc for Orion.

2. Observations and data analysis

The COUP data was obtained during 13 consecutive days in Jan. 2003 with the Advanced CCD Imaging Spectrometer (ACIS) on board the *Chandra* X-ray observatory. The total exposure time is ≈840 ks, separated into 6 observation segments extending over a total time of ≈1140 ks. All observations have the same aimpoint ($\alpha = 5^{\mathrm{h}}35^{\mathrm{m}}17^{\mathrm{s}}$ and $\delta = -5°23'40''$) and the field of view covers an area of $17' \times 17'$; the source COUP 331 is located at $\alpha = 5^{\mathrm{h}}35^{\mathrm{m}}9.2^{\mathrm{s}}$ and $\delta = -5°30'58''$ (cf. Getman et al. 2005). Our analysis is based on the pre-processed photon data provided by the *Chandra* pipeline; for further analysis we applied the CIAO-software in version 3.4. We first screened the photon data for events in the 0.3–13 keV energy band to suppress background. Thereafter, we defined source and background regions as a circle with an 8 arcsec radius and an annulus extending from ≈14–32 arcsec, both centered on the nominal source position.

2.1. The light curve

We generated the background-subtracted 2–9 keV band light curve of COUP 331 shown in Fig. 1. The 6 observation segments can be clearly identified. For most of the COUP observations COUP 331 was recorded at a count rate of 3.3×10^{-3} cts/s, except for two periods. A strong flare (termed "flare I") occurred ≈90 ks after the beginning of the observation. The flare rapidly rises to its peak within ≈4 ks, the decay is again quite rapid with an e-folding time of $\tau_{\mathrm{decay}} = 5.2$ ks, but, unfortunately, is only partially observed. A second, less prominent but very significant count rate enhancement (termed "flare II") occurred 1080 ks after the start of the COUP campaign. This second flare was also not fully covered. Flare II has a much slower rise phase lasting for ≈20 ks, and thereafter, the 2–9 keV band count rate remains more or less constant for at least 40 ks when the COUP observations were terminated. For the rest of the observations COUP 331 was found in quiescence.
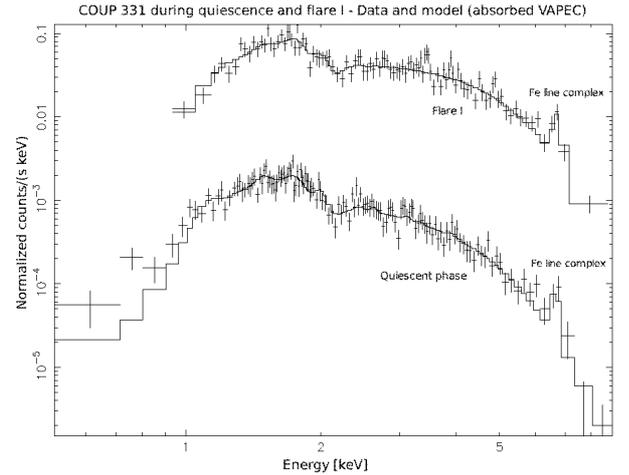
2.2. Spectral analysis

In the following section we carry out temporally resolved spectral analysis of the flare I, flare II, and quiescent phases of COUP 331; note that all quoted errors refer to 90% confidence intervals unless stated otherwise. COUP 331 is located about 7 arcmin off-axis, hence it does not appear as a perfectly symmetric point-source. However, we regard its image distortion as weak and apply the CIAO standard tools for the extraction of point-source spectra (i.e. `psextract`). The spectra were analyzed using the XSPEC environment in version 11.3.1.

2.2.1. The quiescent phase

The quiescent phase spans the 0–1050 ks time interval with the exception of the first flare event, and is the longest lasting phase, covering ≈90% of the total observation time. Note that we disregard a ≈20 ks contribution preceding flare II. During quiescence COUP 331 is detected with a net count-rate of 3.3×10^{-3} cts/s corresponding to an (unabsorbed) X-ray luminosity of 1.6×10^{30} erg/s. We checked for temporal changes in the quiescent spectrum, but did not find evidence for any significant variations. The quiescent X-ray spectrum is well described by an absorbed thin-thermal plasma model (we used the VAPEC models) with all metal abundances – apart from Fe, which is left as a free parameter – fixed to 0.3 times the solar values. In Fig. 2 we show the data and the fit; the best fit model parameters are presented in Table 1, where we list the derived absorbing hydrogen column-density, the temperature, the iron abundance and the fit quality.

2.3. Flare I

For an analysis of flare I we considered all data recorded in the time interval from 87.5 to 102 ks; the spectrum of flare I is shown in Fig. 2. The flare spectrum is very well described by the same model as applied for the quiescent phase (cf. Sect. 2.2.1) with somewhat different spectral parameters listed in Table 1. We find – as expected for a flare – an enhanced temperature of 6.8 keV, leading to a spectrum with a clearly detected Fe line feature at 6.7 keV, but with no detected excess emission at 6.4 keV. From the spectrum we derive an (unabsorbed) peak X-ray luminosity of $L_X = 2.6 \times 10^{32}$ erg/s (in the 1–10 keV band) reached directly after the rise phase, and – with an e-folding time of 5.2 ks for the decay phase – a total energy output of

Table 1. Fit parameters for the absorbed VAPEC model.

Phase	n_H [10^{22} H/cm^2]	Temp. [keV]	Ab$_{Fe}$ [Ab$_\odot$]	χ^2/d.o.f.
Quiescent	$1.09^{1.21}_{0.97}$	$3.0^{3.4}_{2.6}$	$0.32^{0.54}_{0.12}$	131.6/134
Flare I	$1.28^{1.41}_{1.18}$	$6.8^{8.2}_{5.5}$	$0.73^{1.02}_{0.46}$	94.2/99
Flare II	$1.55^{1.66}_{1.41}$	$\gtrsim 13$	$\approx 0.88^a$	102/95

^{a} This value is ill-constrained since temperature-dependent.

$\Delta E \approx 1.4 \times 10^{36}$ erg in the same band. With these numbers, flare I observed on COUP 331 is among the largest stellar flares ever observed.

2.4. Flare II

For the analysis of flare II we considered all data recorded after 1080 ks (cf. Fig. 1). The X-ray spectrum was generated and analyzed in the same fashion as those of the quiescent and flare I phases. From the spectrum of the entire observed flare II phase (see Fig. 3) we calculate an 1–10 keV band X-ray luminosity of 2.4×10^{31} erg/s. Considering a duration of at least 60 ks, the total energy output in this energy band is $\Delta E > 1.4 \times 10^{36}$ erg.

In the fit process of the flare II data we encountered two problems. First, the absence of temperature-sensitive features in the spectrum – especially the hot Fe XXV feature at 6.7 keV and its Fe XXVI counterpart near 7 keV – prevents us from tightly constraining the plasma temperature. We find that any choice of the temperature beyond 10 keV leads to acceptable fits, and thus decided to apply a value of 13 keV. Second, the spectrum shows definite excess emission above the thermal continuum at 6.4 keV, which we attribute to the Fe I K$_\alpha$ line. We therefore included an additional instrumentally broadened Gaussian component centered at 6.4 keV into our model and refitted, leaving only the normalization of the Gaussian component free to vary. The thus obtained fit is shown in Fig. 3, which shows the obvious presence of the 6.4 keV line and virtual absence of the 6.7 keV Fe XXV feature. The resulting fit parameters for the thermal model are again listed in Table 1, and for the Gaussian component we arrive at a normalization of $5(3.3–6.7) \times 10^{-6}$ ph/(cm^2 s), corresponding to an equivalent width of 685(452–918) eV. As is obvious from Fig. 3, the inclusion of a Gaussian component at 6.4 keV into the model significantly increases the fit quality.

As a first result we thus note that the 6.4 keV emission feature is present – at best – only during 60 ks during flare II. In order to further temporally constrain the presence of the 6.4 keV iron line we constructed a background-subtracted 6.1–6.7 keV narrow-band light curve of COUP 331 with a 4 ks binning in addition to the 2 ks binned 2–9 keV band light curve; both light curves are shown in Fig. 4. As is clear from Fig. 4 the 2–9 keV band light curve stays more or less constant after the rise to peak, while the 6.1–6.7 keV narrow-band light curve decays quite rapidly. We therefore subdivided the the flare II phase data into three consecutive 20 ks time intervals, denoted by "rise-phase", "phase II", and "phase III" as indicated in Fig. 4. The X-ray spectra in the 5–8 keV region corresponding to these time intervals are shown in Fig. 5. In these plots the solid line indicates the thermal model described earlier. For all spectra the same model was applied, but we allowed the normalizations of the VAPEC and Gaussian component to be fitted independently for all time intervals; all other parameters were regarded globally. Figure 5 clearly demonstrates an evolution of the
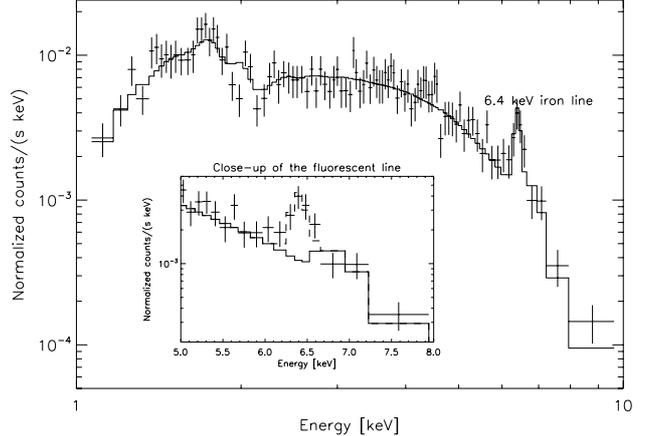

Fig. 3. The COUP 331 spectrum during flare II with a close-up of the 5–8 keV energy band. Two model fits are indicated. First, (solid line) an absorbed thermal model and second (dashed line), the same thermal model with additional instrumentally-broadened Gaussian component centered at 6.4 keV.
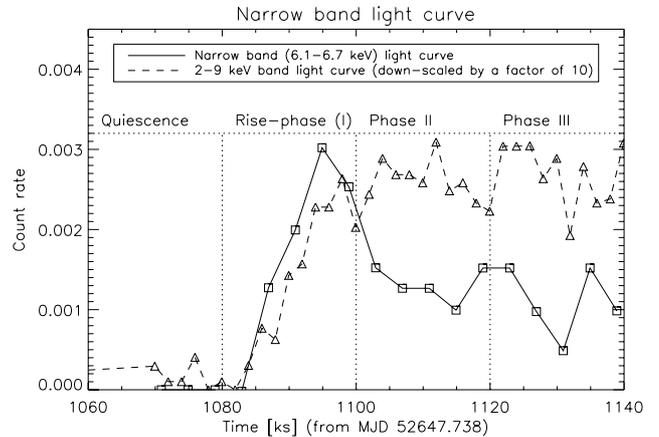

Fig. 4. The background-subtracted narrow-band light curve (solid line) of COUP 331 during the last 80 ks of the COUP observation. The light curve peaks in the rise-phase of flare II. For clarity the 2–9 keV light curve is also shown (dotted line – scaled to fit the plot range).

Fe I K$_\alpha$ line strength. Interestingly the line normalization decreases as time proceeds, while the underlying thermal spectrum remains almost unaffected. We thus interpret the variations in the narrow-band light curve shown in Fig. 4 as arising from variations in the Fe I K$_\alpha$ feature's strength. Note that the constancy of the thermal spectrum does not imply the same for the temperature, since the latter exceeds 10 keV, producing a flat spectrum in the "low energy" band we are observing. The K$_\alpha$ feature is strongest during the flare II rise phase where our fits yield a line flux of $9.1(5.8–13.4) \times 10^{-6}$ ph/(cm^2 s) (an EW of ≈ 1400 eV) while in phase II and III it is reduced to 3.04(0.8–7.6) and $0.9(0–4.8) \times 10^{-6}$ ph/(cm^2 s), respectively. This is also reflected by the narrow-band light curve around 6.4 keV (cf. Fig. 4).

3. Interpretation and conclusions

Our time resolved analysis of the COUP X-ray data of the YSO COUP 331 shows that for $\approx 90\%$ of the entire observation time the object is found in a quiescent state characterized by an X-ray temperature of 30–40 MK. Two major flares are covered by the COUP observation. In the first data segment a relatively short duration event with a peak X-ray luminosity of
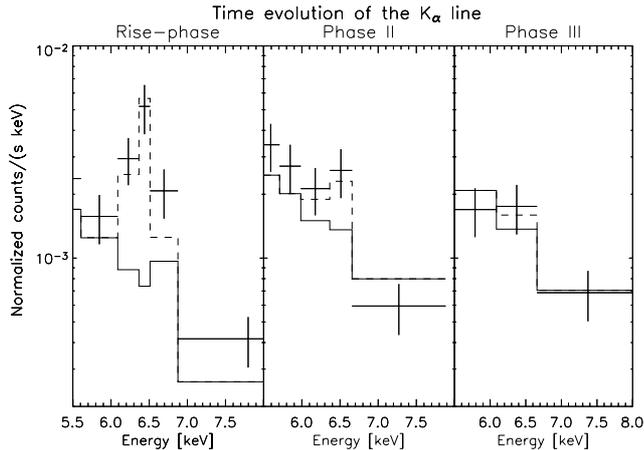
Fig. 5. Time-resolved 5.5−8 keV section of the COUP 331 spectrum (cf. Fig. 4). Note the decrease of the Fe I K$_\alpha$ line's strength.

2.6×10^{32} erg/s occurred, which clearly shows the 6.7 keV iron feature, but no Fe I K$_\alpha$ emission.

In the last COUP data segment a long duration flare event occurred; starting with a ≈ 20 ks rise phase it lasted >60 ks. The decay of this flare cannot be constrained because the COUP observations were stopped. The total amount of energy released in the $1-10$ keV energy band is $>1.4 \times 10^{36}$ erg; the X-ray temperature of this flare is extremely large ($\gtrsim 10$ keV) and can in fact not be well constrained with the *Chandra* data. A clear and highly significant detection of the fluorescent K$_\alpha$ line is obtained only during the 20 ks rise time of this flare; at later times the line may still be present albeit at a lower level. This event on COUP 331 resembles a huge flare observed on Algol, observed by Favata & Schmitt (1999) with BeppoSAX, which also shows a slow rise phase, followed by a nearly constant phase – lasting for ≈ 80 ks – in its $1.6-10$ keV band light curve. However, the corresponding $15-100$ keV band light curve clearly shows the characteristics of a decay phase (cf., Favata & Schmitt 1999, Figs. 1 and 2). The energy output of 1.4×10^{37} erg derived by Favata & Schmitt (1999) in the $0.1-10$ keV band compares well to the numbers estimated for COUP 331, note however that no Fe I K$_\alpha$ line was detected.

The precise temporal association between Fe I K$_\alpha$ line emission and high energy continuum is necessary in order to quantitatively assess the origin of the Fe I K$_\alpha$ emission observed in COUP 331; we find that the actual photon flux in the fluorescent K$_\alpha$ line during the flare II rise phase is 35 times larger than reported by Tsujimoto et al. (2005). This discrepancy arises because Tsujimoto et al. (2005) give time-averaged values, whereas our values refer to several limited time intervals. The X-ray temperature during the flare event was extremely large; the total luminosity in the Fe I K$_\alpha$ line alone is $\approx 2.3 \times 10^{30}$ erg/s. While these circumstances appear to favor the excitation of the Fe I K$_\alpha$ line through photoionization, preliminary model calculations challenge such a scenario. We repeated the calculations carried out by Bai (1979) applying a reflector with cosmic abundances. We used the same branching ratios and cross sections for iron, but slightly different cross section for absorption by other elements composed according to cosmic abundances. Furthermore, we located the source directly on the reflector to make it subtend half the sky, thus providing an upper limit for the fluorescent iron line flux. The illuminating input spectrum was modeled as a thermal X-ray spectrum with a temperature of 13 keV, normalized to the measured fluxes. Our preliminary calculations show that an already optimally assumed fluorescence geometry significantly underpredicts the observed Fe I K$_\alpha$ flux, making an interpretation of the Fe I K$_\alpha$ line through photoionization difficult to accept. However, these calculations will be extensively discussed in a larger and systematic context in a forthcoming paper, where we will also address its impact on the characteristics of COUP 331 and other sources with fluorescent K$_\alpha$ emission.

References

Bai, T. 1979, Sol. Phys., 62, 113
Fabian, A. C., Rees, M. J., Stella, L., & White, N. E. 1989, MNRAS, 238, 729
Favata, F., & Schmitt, J. H. M. M. 1999, A&A, 350, 900
Favata, F., Micela, G., Silva, B., Sciortino, S., & Tsujimoto, M. 2005, A&A, 433, 1047
Getman, K. V., Flaccomio, E., Broos, P. S., et al. 2005, ApJS, 160, 319
Herbst, W., Bailer-Jones, C. A. L., Mundt, R., Meisenheimer, K., & Wackermann, R. 2002, A&A, 396, 513
Imanishi, K., Koyama, K., & Tsuboi, Y. 2001, ApJ, 557, 747
Neupert, W. M., Gates, W., Swartz, M., & Young, R. 1967, ApJ, 149, L79
Stassun, K. G., Mathieu, R. D., Mazeh, T., & Vrba, F. J. 1999, AJ, 117, 2941
Tanaka, Y., Nandra, K., Fabian, A. C., et al. 1995, Nature, 375, 659
Tsujimoto, M., Feigelson, E. D., Grosso, N., et al. 2005, ApJS, 160, 503
Zarro, D. M., Dennis, B. R., & Slater, G. L. 1992, ApJ, 391, 865